The Estimation of Wind-Wave Generation in a Discrete Spectral Model

DONALD T. RESIO

U.S. Army Engineer Waterways Experiment Station, Vicksburg, MS 39180

(Manuscript received 15 October 1979, in final form 5 December 1980)

ABSTRACT

The estimation of wind-wave generation using a new discrete spectral model is compared to Hasselmann *et al.*'s (1976) parametric model and to models driven primarily by direct transfer of energy from the atmosphere into the surface waves. The main source term in this new model is a new parameterization of the net energy transfer due to nonlinear wave-wave interactions. After calibration of the wave-wave interaction source term to resemble the form of the solution to the complete Boltzmann integrals, the discrete spectral model is able to reproduce the fetch-limited results of Hasselmann *et al.* and fits well within the envelope of duration-limited growth curves from recent investigations. Since this model is discretized into frequency and direction components, a finite-difference scheme is used to model propagation effects. The formulation of this model allows simulations in oceanic conditions to consider both wave growth under local winds and swell decay of waves passing through a region simultaneously.

1. Introduction

Hasselmann *et al.* (1976) introduced a parametric model of wind-wave generation, relating the rate of change of a single nondimensional wave parameter to nondimensional characteristics of the wind field. Prior to that, since the mid 1960's, most models of wind-wave generation, propagation and dissipation had been formulated in terms of solutions of relevant equations for individual frequency-direction components of the spectrum (Pierson *et al.*, 1966; Barnett, 1968; Ewing, 1971). In a review of numerical wave prediction technology, models of this latter type have been termed discrete spectral models by Cardone and Ross (1977). To date, there has been little effort to document significant differences among various methods of predicting waves in deep water and it is most often assumed that the various methods produce similar results when correctly applied. However, the results of comparisons by Dexter (1974) and Resio and Vincent (1979) indicate that, while this might be true for waves in their late stages of development, significant discrepancies arise among these methods for the cases of fetch-limited waves and duration-limited waves in their early stages of development. The purpose of this paper is to discuss ramifications of different concepts of wave generation in terms of comparisons to observations and to develop a general scheme for a discrete spectral model which can produce results in good agreement with these observations.

Results of the Joint North Sea Wave Project (JONSWAP) indicate that wave growth along a fetch is governed by a self-similar process. In that study the dominant energy input on the forward face of the spectrum is related to a convergence of energy flux due to nonlinear, resonant wave-wave interactions of the form as described by Hasselmann (1962). The results of Mitsuyasu (1968, 1969) also show a pattern of spectral wave growth along a fetch as was first described by Kitaigorodskii (1962). Well before Kitaigorodskii's work, however, investigators in the late 1940's (Sverdrup and Munk, 1947) were proposing relationships among nonspectral wave parameters, wind speeds, fetches and durations based on dimensional considerations and empirical evidence. One of these, formalized by Kitaigorodskii (1962) and well substantiated in the Hasselmann *et al.* (1973) and Mitsuyasu (1968, 1969) studies, is that the growth of wave height H along a fetch should be representable in the form

$$\tilde{H} = m_1\tilde{X}^{m_2}, \quad (1)$$

where m_1 and m_2 are two universal constants for the case of deep water and $\tilde{H}$ is a nondimensional wave height defined as $\tilde{H} \equiv g(E_0/u^2)^{1/2}$, where g is the gravitational acceleration, E_0 is the total wave energy and u is the wind velocity at some reference level. $\tilde{X}$ is a nondimensional fetch defined by $\tilde{X} \equiv gx/u^2$, where x is the distance along the fetch.

In the absence of significant refraction, shoaling and diffraction, the radiative transfer equation for surface gravity waves is reduced to

$$\frac{\partial F(x,y,t,f,\theta)}{\partial t} = G(x, y, t, f, \theta) - \mathbf{c}_g(f, \theta)\cdot\nabla\mathbf{F}(x, y, t, f, \theta), \quad (2)$$

where F is the energy density of the spectral element located on the water surface at point (x, y) at time t with frequency f and direction of propagation θ, G is the rate of transfer of wave energy into or out of this spectral element, and $\mathbf{c}_g(f, \theta)$ is the group velocity associated with this element. Pierson *et al.* (1966, hereafter referred to as PTB), as discussed in Pierson (1977) assume that the effects of wave-wave interactions, if they do become significant, do so only in late stages of wave development, in which case these effects are implicitly modeled by including a limiting form for wave development in Eq. (2). Hasselmann *et al.* (1973, 1976) and Weare and Worthington (1978) take the contrasting position that nonlinear terms dominate the source mechanism to such an extent that the pattern of growth of the wave spectrum and the constancy of spectral shape represents an equilibrium with local wind and wave scaling parameters. Thus, they believe that parametric models yield a more accurate description of wave growth.

The PTB method uses a form for the source mechanisms which follows from the original theoretical developments of Phillips (1957) and Miles (1957). This approach treats individual spectral elements as though they were uncoupled and receive essentially all of their energy from direct atmospheric transfer, i.e.,

$$G_{\mathrm{PTB}} = A_2 + B_2F, \tag{3}$$

where F is the same as in Eq. (2) without explicitly denoting here the dependence on x, y, t, f and θ. A_2 and B_2 represent separate atmospheric source terms, both considered to be functions only of wave frequency, propagation angle relative to wind direction and wind speed. Recent attempts to measure direct energy fluxes into the wave field from the atmosphere have indicated that most of this transfer occurs in the central band of energy containing frequencies and not on the forward face of the spectrum (Dobson, 1971; Wu *et al.*, 1979). Of practical significance is the question as to whether or not this $A + BF$ source configuration can produce results in approximate agreement with observations, in spite of the fact that they may not represent actual physical source terms.

On the other hand, Hasselmann *et al.* (1973, 1976) suggest that simple parameterizations of wave-wave interactions, such as proposed by Barnett (1968) and Ewing (1971), although they are quite accurate for Pierson-Moskowitz spectra do not suffice to provide reliable results when applied in numerical wave prediction schemes. They conclude, instead, that such parameterizations should include a more sophisticated treatment of various shape factors of the spectrum. This conclusion would appear to be borne out by comparisons made in Fig. 1, at least relative to the Barnett parameterization. These comparisons between the computed solution of the Boltzmann integrals describing the transfer of energy due to nonlinear wave-wave interactions and Barnett's parameterization of this transfer show that this type of three-parameter representation is not accurate for a broad range of spectral shapes. What is needed then is a new parameterization of the wave-wave interaction source terms, one which does give a good approximation to the evaluation of the Boltzmann integrals.

2. Parameterization of nonlinear wave-wave interactions

Webb (1978) provides good insight into the wave-wave interaction process taken by Hasselmann *et al.* (1973, 1976) to be responsible for most energy transfer into spectral elements on the forward face of the spectrum. He conceptualizes the process as being made up of two related transfers; one which is termed "diffusive" since it transfers energy down an energy gradient and a second which is termed "pumped" since it represents that transfer required to accompany the diffusive transfer in order to conserve energy, momentum and action. The term pumped was chosen by Webb in order to emphasize the analog of this transfer process to other systems in which entropy is locally decreased in a particular region at the expense of an increase in entropy elsewhere. Given four wavenumbers $\mathbf{k}_1, \mathbf{k}_2, \mathbf{k}_3, \mathbf{k}_4$, and associated action densities n_1, n_2, n_3, n_4, Webb defines the pumped and diffusive transfers under the constraint $|\mathbf{k}_1 - \mathbf{k}_3| < |\mathbf{k}_1 - \mathbf{k}_4|$, as

$$\frac{dn}{dt}\,(\text{pumped}) = 2 \iiiint\!\!\iint C(\mathbf{k}_1, \mathbf{k}_2, \mathbf{k}_3, \mathbf{k}_4)\delta(\mathbf{k}_1 + \mathbf{k}_2 - \mathbf{k}_3 - \mathbf{k}_4)\delta(\omega_1 + \omega_2 - \omega_3 - \omega_4) \times \zeta(|\mathbf{k}_1 - \mathbf{k}_4| - |\mathbf{k}_1 - \mathbf{k}_3|)n_1n_3(n_4 - n_2)\mathbf{dk}_2\mathbf{dk}_3\mathbf{dk}_4 \tag{4a}$$

and

$$\frac{dn}{dt}\,(\text{diffusive}) = 2 \iiiint\!\!\iint C(\mathbf{k}_1, \mathbf{k}_2, \mathbf{k}_3, \mathbf{k}_4)\delta(\mathbf{k}_1 + \mathbf{k}_2 - \mathbf{k}_3 - \mathbf{k}_4)\delta(\omega_1 + \omega_2 - \omega_3 - \omega_4) \times \zeta(|\mathbf{k}_1 - \mathbf{k}_4| - |\mathbf{k}_1 - \mathbf{k}_3|)n_2n_4(n_3 - n_1)\mathbf{dk}_2\mathbf{dk}_3\mathbf{dk}_4, \tag{4b}$$

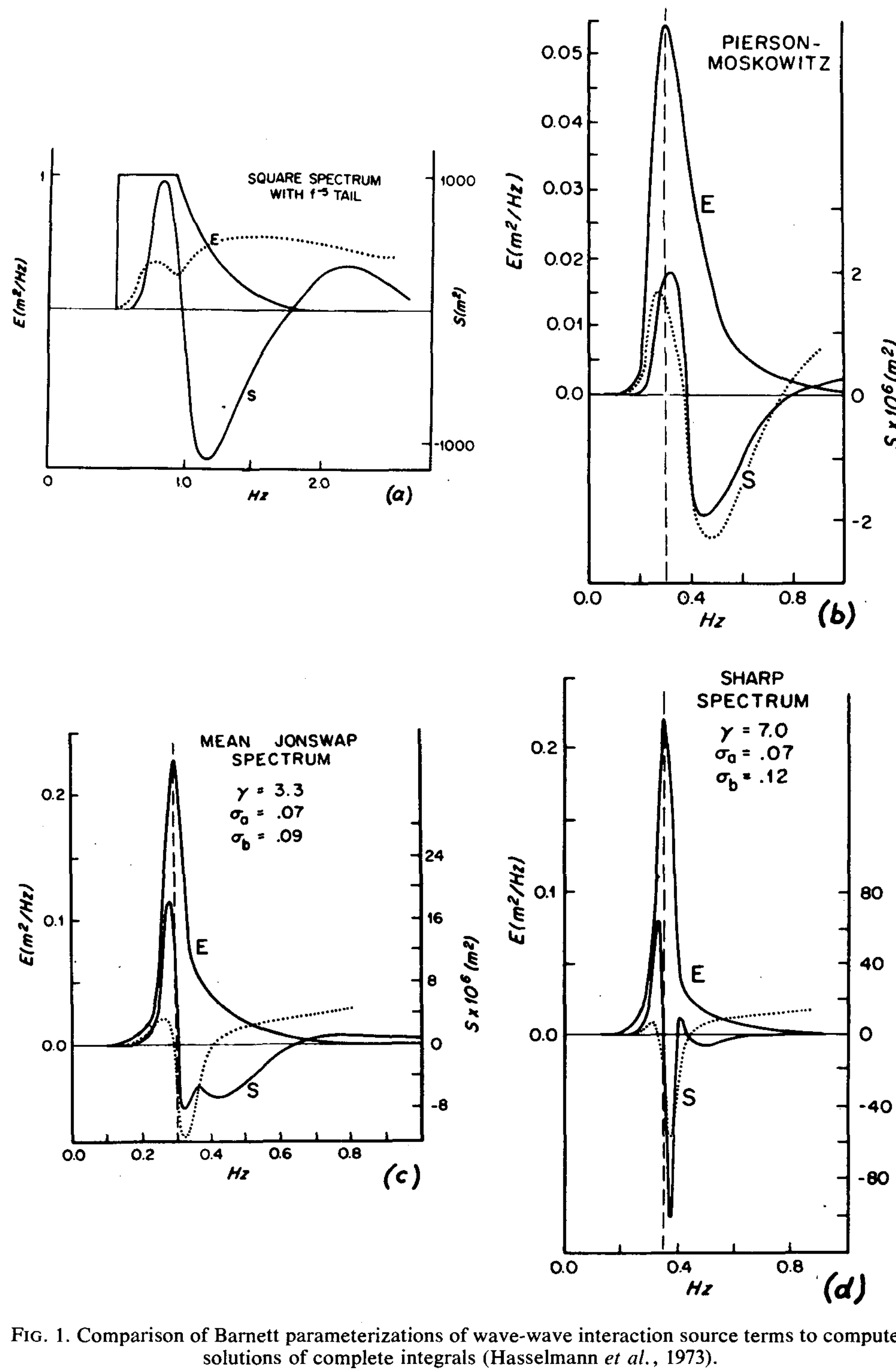

FIG. 1. Comparison of Barnett parameterizations of wave-wave interaction source terms to computed solutions of complete integrals (Hasselmann *et al.*, 1973).

where the delta functions of wavenumbers and angular frequencies are present to insure conservation of momentum and energy, respectively, and the ζ function is 1 when the argument is positive and 0 otherwise. The term C is the coupling coefficient which dictates the rate at which interactions occur. Appendix 1 in Webb (1978) gives a representation of this algebraically complex function for the case of deep water.

As seen in Fig. 1, the general form for the net transfer of energy within a spectrum is given by three lobes, a positive source located on the forward face, a negative source located at frequencies slightly above the spectral peak and another positive source at still higher frequencies. In the problem of numerical wave prediction, only the first two lobes are important since the energy transfer into the third lobe is at such frequencies that viscous and turbulent dissipation is assumed to keep the local energy density small.

Although it is easier to treat the mathematics for the complete solution in terms of action density, most wave prediction is carried out in terms of energy densities. Since $n(\mathbf{k}) = F(\mathbf{k})/\omega$, where $\omega = g|\mathbf{k}|$, a straightforward transformation can be used to obtain arguments in terms of $F(\mathbf{k})$ or $F'(f, \theta)$ for a parameterization. Observational evidence is given most often as a one-dimensional energy density $E(f)$, thus, the latter form $F'(f, \theta)$ is preferred here. In this paper, we shall restrict our attention to spectra of the form

$$F'(f, \theta) = E(f)Z(\theta),$$

where Z is a symmetric function around θ_0, the mean direction of wave propagation. The form of Eqs. (4a) and (4b) is such that, if the initial spectrum is symmetric about θ_0, net energy transfers will maintain this symmetry. If one considers the dimensions of all terms involved in Eqs. (4a) and (4b) and limits the shape of $E(f)$ to a single peak, then a reasonable scaling for interactions on the forward face of the spectrum (the first lobe) will be of the form

$$\frac{\partial E(f)}{\partial t} \sim \langle E(f)\rangle^2_{(+)} \left\langle \frac{\partial E(f)}{\partial f} \right\rangle_{(-)} C'(f_0)\psi\left(\frac{f}{f_m}\right), \quad (5)$$

where the angle brackets denote an averaging process over that region of the spectrum characterizing the positive and negative lobes of the net transfer, and ψ is a nondimensional function of relative frequency f/f_m. The $C'(f_0)$ term is related to the coupling coefficient in Eqs. (4a) and (4b). As pointed out by Webb (1978) for deep-water waves $C(b\mathbf{k}_1, b\mathbf{k}_2, b\mathbf{k}_3, b\mathbf{k}_4) = b^6C(\mathbf{k}_1, \mathbf{k}_2, \mathbf{k}_3, \mathbf{k}_4)$, thus since $f \sim k^{1/2}$, then $C'(f_0) \sim f_0^{12}$. In Eq. (5), f_0 functions as a frequency scale taken here to be that frequency located at the point of contact between the first and second lobes of the net transfer function.

For the case of the growing sea, if the modulation of the "overshoot-undershoot" effect (Barnett and Sutherland, 1968) is neglected, the energy density in the region of the spectrum where the negative lobe of the interaction transfer is located is given by

$$E(f) = \alpha g^2(2\pi)^{-4}f^{-5}. \quad (6)$$

On the forward face of the spectrum, the energy density is approximated by $E(f_m)\psi(f/f_m)$. Combining these relationships into Eqs. (5) and (6) yields

$$\frac{\partial E(f)}{\partial t} = D_1\alpha^3g^2f_m^{-4}\psi\left(\frac{f}{f_m}\right), \quad (7)$$

where D_1 is a nondimensional constant. In this instance, the proper scaling frequency f_0 is taken as f_m. In Barnett (1968) and Ewing (1971) the scaling frequency f_0 is represented as the mean frequency of the spectrum

$$f_0 \equiv E_0^{-1} \int_0^\infty E(f)fdf.$$

For an f^{-5} spectrum with a steep forward face, $f_0 \approx \frac{4}{3}f_m$. As long as these two frequencies are linearly related, there is no fundamental difference between using either scale for a self-similar spectrum. If we examine Figs. 1c and 1d, the intersection of the positive and negative interaction nodes occurs, for practical purposes, at f_m, in agreement with its usage here; and there is little difference between using f_m or Barnett's f_0 as a scaling frequency. On the other hand, in case *a* the location of f_m is not well defined; and in case *b* the location of f_m does not coincide with f_0. Clearly, neither f_m nor Barnett's f_0 is a fundamental scaling parameter for all spectral shapes.

The null-point between positive and negative transfers occurs in the middle range of frequencies in a spectrum when the convergence of energy transfer in the pumped term (4a) is exactly balanced by divergence of energy transfer in the diffusive term (4b). From dimensional considerations and the functional dependencies of the pumped and diffusive terms, it can be inferred that this point will be located in the neighborhood of a frequency such that

$$\frac{\partial}{\partial f}\left[E^2(f)\,\frac{\partial E(f)}{\partial f}\,C'(f)\right] = 0 \quad (8)$$

given that the spectrum is unimodal. If the local derivative of the spectral density is given by

$$\frac{\partial E(f)}{\partial f} = qf^{-(n+1)}, \quad (9)$$

then (8) will be met when $n = 3\frac{2}{3}$. For $n < 3\frac{2}{3}$, the diffusive term will dominate and energy will diverge from this region. For $n > 3\frac{2}{3}$, the pumped transfer will begin to dominate and energy will converge toward this region. Consequently, this criterion will be taken for the definition of f_0 in Eq. (5).

It is important to note that Eq. (8) is not intended to imply that $\partial S_{nl}/\partial f = 0$ at f_0, but rather that f_0 is located at the point in which the rate of change of the scaling function with respect to frequency is equal to zero.

For a range of peak frequencies from 0.05 to 0.4, the value of f_0 determined in this way is about $1.24f_m$ for a Pierson-Moskowitz (PM) spectrum, given by

$$E(f) = \alpha g^2(2\pi)^{-4}f^{-5}\exp[-0.74(f_m/f)^4], \quad (10)$$

where the substitution $f_m = g/u$ has been made into the original equation proposed by Pierson and Moskowitz (1964). In Fig. 1b, the value of f_m is 0.30 and the value of $f_0 \approx 0.38$, which compares favorably with that predicted from the relationship proposed here. This parameterization of f_0 is best suited for spectra with monotonic derivatives of energy density with respect to frequency. If there are several points at which n in Eq. (9) equals $3\frac{2}{3}$, it is unclear at present whether or not each will function as an f_0 with several positive and negative lobes distributed throughout the spectrum or whether the different lobes would blend together. It is expected that this behavior will depend on the separation between those f_0 points, relative to the width of the expected transfer lobes. From the shape of the exact solutions shown in Fig. 1, it appears that the form and intensity of the energy transfers are largely related to the levels of the spectrum near the spectral peak. A spectral width parameter such as the root mean square frequency deviation to either side of f_m can be used to characterize this distribution.

3. Discrete spectral parameterization of wave growth

Fig. 2 shows a comparison of three spectral shapes: a PM spectrum [given by Eq. (10)], a JONSWAP spectrum given by

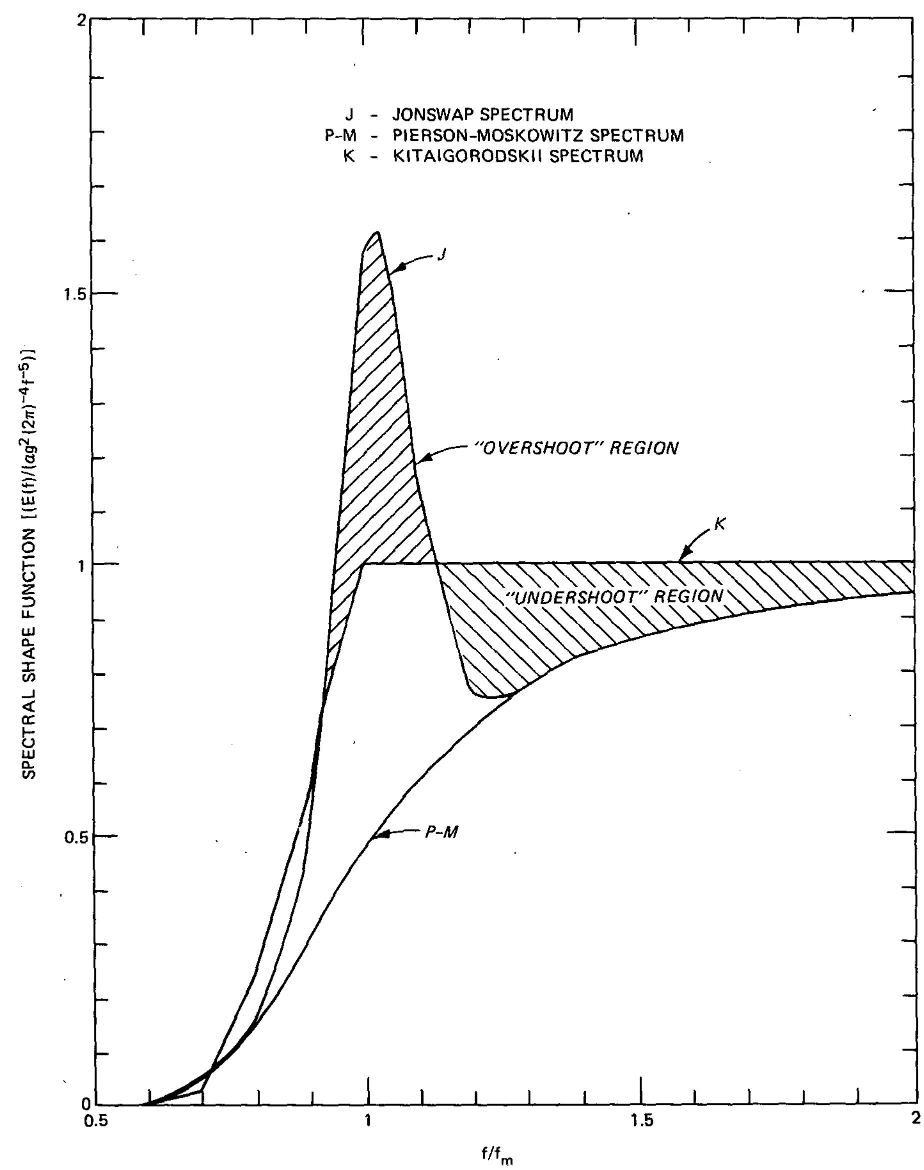

FIG. 2. Comparison of nondimensionalized shapes of spectra proposed by Kitaigorodskii (1962) (K), Hasselmann *et al.* (1973) (J) and Pierson and Moskowitz (1964) (PM).

$$E(f) = E_{PM}(f)\delta^{\exp[-(f-f_m)^2/(2\sigma^2 f_m^2)]}, \quad (11)$$

where $\sigma = 0.07$ for $f < f_m$, $\sigma = 0.09$ for $f \geq f_m$, $\delta = 3.3$, and a Kitaigorodskii-type of spectrum is given by

$$E(f) = \begin{cases} \alpha g^2 f^{-5}(2\pi)^{-4}, & f \geq f_m, \\ \alpha g^2 f_m^{-5}(2\pi)^{-4} \times \exp[1 - (f_m/f)^4], & f < f_m. \end{cases} \quad (12)$$

In essence, the PM spectrum has only one free parameter f_m, since everything else in Eq. (10) is a constant, whereas the spectra from Eqs. (11) and (12) contain two free parameters f_m and α. Fig. 2 represents the comparison when $\alpha = 0.0081$, the value taken as a universal constant in the PM spectrum. As can be seen here, the spectra given by (11) and (12) are quite similar in terms of total energy, with the JONSWAP spectrum showing more evidence of the overshoot-undershoot oscillation around the saturation energy in the equilibrium range. Since, the concentration of energy near the spectral peak can be important in many applications, this similarity in total energy does not imply the two spectral shapes may be used interchangeably.

In a numerical model of the discrete spectral type, the information on spectral shape is not sufficient to merit a laborious calculation of derivatives, moments, etc. Consequently, a parameterization of the nonlinear source term G_{NL} that is stable and still retains characteristics of the Kitaigorodskii-type spectrum can perhaps best be formulated in terms of Eq. (7). On the forward face of the spectrum, the function $\psi(f/f_m)$ must be related to the spectral width, which for spectra given by Eq. (12) leads to

$$G_{NL} = D_1\alpha^3 g^2 f_m^{-4} \exp[1 - (f_m/f)^4](f/f_m)^3. \quad (13)$$

For now, let us assume that the level of energy in the so-called equilibrium range is governed by an instantaneous balance among the wave-wave interaction sink, wave breaking and the atmospheric input. Several studies (Mitsuyasu, 1968; Hasselmann *et al.*, 1973, 1976) have indicated that there is a relationship between α and nondimensional fetch of the type

$$\alpha = m_3\tilde{X}^{m_4}, \quad (14)$$

where m_3 and m_4 are universal constants. However, in a numerical model, the concept of fetch in a time-varying, space-varying windfield is quite ambiguous and subjective. An easier nondimensional relationship to apply can be formulated in terms of nondimensional wave height

$$\alpha = m_5\tilde{H}^{m_6}, \quad (15)$$

where m_5 and m_6 are two new constants. Alternatively, a nondimensional peak frequency, defined as $\tilde{f}_m = uf_m/g$, could be used to estimate α. From the JONSWAP study we have

$$\alpha = 0.076\tilde{X}^{-0.22},$$

$$\tilde{f}_m = 3.5\tilde{X}^{-0.33}.$$

Substituting these relationships into Eq. (13) yields

$$G_{NL} = D_2 g^6(u/f_m)^2 \exp[1 - (f_m/f)^4](f/f_m)^3 \quad (16)$$

which is interesting since it demonstrates how such a wave-wave interaction source term can behave as an apparent wind source term. Without the variation of α implicit in the functional relation between α and some wave parameter nondimensionalized by wind speed, this would not be possible. The fact that the wind speed enters into Eq. (16) as a squared term is reassuring in a physical context since the transfer of momentum due to surface stress is expected to be of the form $\tau = C_D u$, where C_D is the coefficient of drag. The parameterization of G_{NL} here is fundamentally different than those proposed by Barnett (1968) and Ewing (1971). Neither of those contain any factor which will produce the wind speed dependence reported here, given that both previous models were formulated to work with the assumption that α is a constant.

An equivalent relationship to Eq. (16) can be formulated in terms of nondimensional wave height if the relationship shown in Eq. (15) is used with $m_6 = -0.47$. A comparison of this relationship with observational evidence is shown in Fig. 3. This method is preferred over the use of nondimensional peak frequency for estimating α in a numerical model since the total energy is estimated with more precision than the location of the spectral peak.

For a fixed wind speed, the variation of α with E_0 is small. Thus, the rate of growth is essentially given by

$$\frac{\partial E_0}{\partial t} \approx \int_0^{f_0} G_{nl} df \quad (17)$$

or along a fetch by

$$\frac{\partial E_0}{\partial x} \approx \int_0^{f_0} G_{NL}\bar{c}_g^{-1} df, \quad (18)$$

provided that the angular distribution of the energy density is reasonably constant and that $\bar{c}_g$ is the average component of propagation in the positive fetch direction [$=0.85c_g$ for $Z(\theta) = \cos^2(\theta - \theta_0)$]. Combining Eqs. (16) and (18) and noting that for the type of spectrum considered here $f_0 = f_m$,

$$\frac{\partial E_0}{\partial x} \approx D_3 g^{-1} f_m^{-2} u^2 \int_0^{f_m} f \exp(f_m/f)^4 df$$
$$\approx D_4 u^2 g^{-1}, \quad (19)$$

where D_3 and D_4 are dimensionless constants. It is

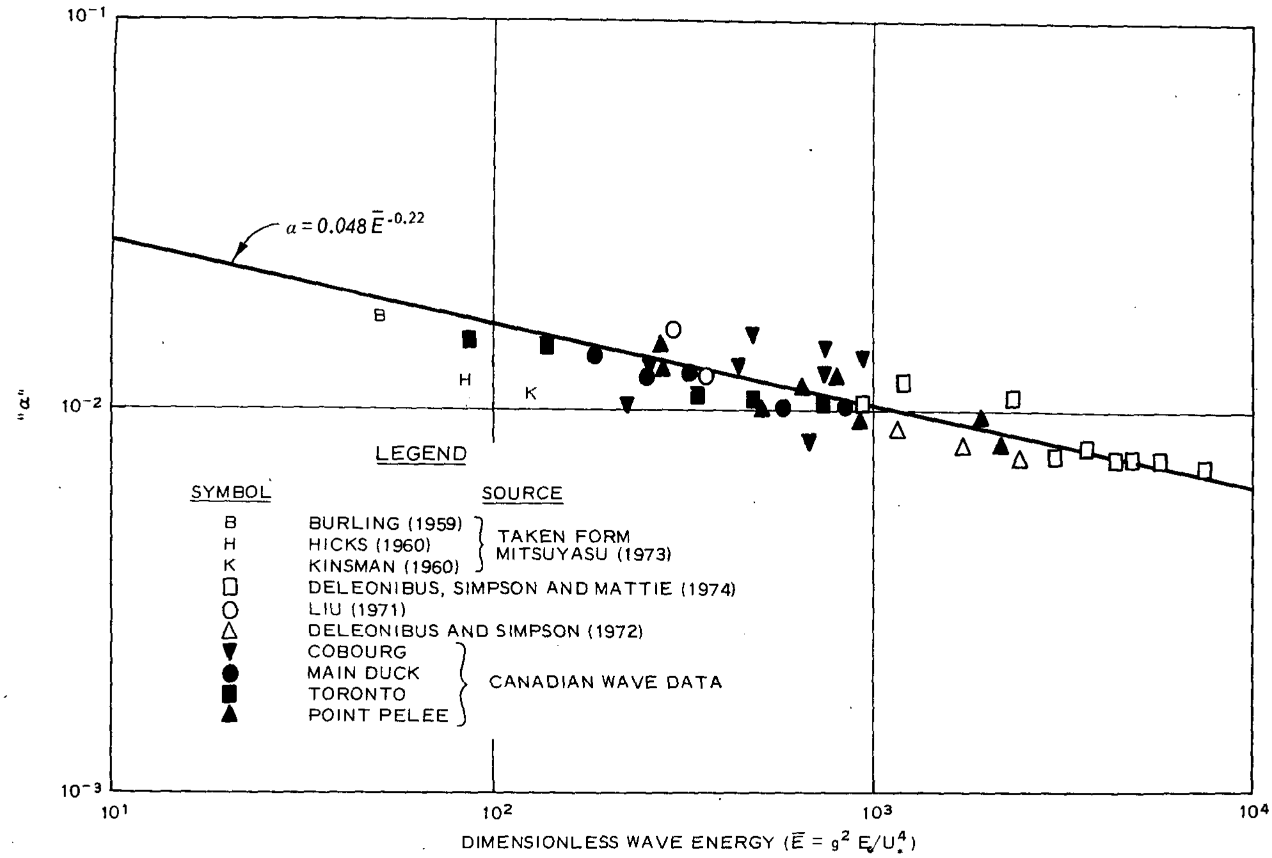

FIG. 3. Relationship between Phillips equilibrium coefficient α and nondimensional wave energy (after Resio and Vincent, 1977a).

apparent here that the rate of growth of total energy along a fetch is a constant, independent of x. From the JONSWAP data, we have $\tilde{E}_0 = m^7\tilde{X}$ where $\tilde{E} = \tilde{H}^2$. Hence in dimensional terms

$$E_0 = m_7 u^2 x/g, \tag{20}$$

$$\frac{\partial E_0}{\partial x} = m_7 u^2/g. \tag{21}$$

Clearly, if $D_4 = m_7$, then the growth of total energy in a model based on the form of G_{NL} proposed here will correspond to that observed by Hasselmann *et al.* (1973). Since the spectral formulation used here is based on that of Kitaigorodskii (1962), wave growth follows a self-similar pattern, in agreement with the JONSWAP data although with a somewhat different shape as seen in Fig. 2. The question now arises as to whether or not a model with $A + BF$ source terms can reasonably duplicate these results.

4. Spectral growth with $A + B$ source terms

Most of the empirical calibrations of the A and B source functions have relied on one-dimensional spectral information. For simplicity, the two-dimensional source functions in Eq. (3) will be assumed to have an equivalent one-dimensional representation $A_1 + B_1E(F)$ that will produce essentially the same pattern of spectral wave growth as the $A_2 + B_2F$ source terms integrated over direction. Although several forms for B_1 have been proposed, most of these can be reduced to a nondimensional relationship of the form (Snyder and Cox, 1966; Barnett, 1968; Lazanoff and Stevenson, 1975; Dobson and Elliot, 1977)

$$B_1/f = \phi(u/c), \tag{22}$$

where c is the phase velocity of a spectral element with frequency f. For a self-similar spectrum of the Kitaigorodskii type, on the forward face we have along a fetch

$$\int_0^{f_m} \frac{B_1E(f)df}{c_g} = \frac{2\alpha g f_m^{-5}}{(2\pi)^3}\int_0^{f_m} f^2\psi\left(\frac{f}{f_m}\right)\phi(u/c)df. \tag{23}$$

If we allow $\phi(u/c) \sim (u/c)^n$ then Eq. (23) becomes

$$\int_0^{f_m} B_1E(f)df = m_{12}f_m^{n-2}, \tag{24}$$

which can be calibrated into a constant function of wind speed, as in Eq. (19), only for the case $n = 2$. However, most of the theoretical and empirical studies have led to the use of forms for B_1 with $n = 1$ (Synder and Cox, 1966; Barnett, 1968; Lazanoff and Stevenson, 1975; Dobson and Elliot, 1977). Additionally, the behavior of α would not be properly modeled with such an approach. If the JONSWAP relationship for a given wind speed, $\alpha \sim f_m^{2/3}$, is applied then the exponent in (24) becomes $n - 4/3$, which when the usual factor $n = 1$ is substituted into it yields only a weak dependence on f_m.

Since the A_1 and B_1 terms are not functionally equivalent, the A term must independently approach a constant when integrated over the range of growing frequencies, for waves generated along a fetch. A typical dependence of A on frequency is of the form $A \sim f^{-n}$ for frequencies up to the peak of the fully developed spectrum for a given wind speed. Thus the growth of total energy due to this source along a fetch is

$$\frac{\partial E_0}{\partial x} = m_{12} \int_0^{f_m} f^{1-n} df. \qquad (25)$$

For $n = 2$, the growth of total energy depends on $\ln f_m$; and for $n \neq 2$, it depends on f_m^{2-n}. This seems to suggest that such a source term, i.e., a linear source term not dependent on the relative location of the spectral peak, cannot be significant in the growth of waves along a fetch. This may explain some of the necessity of recalibrating models with $A + B$ source terms when applying them to regions dissimilar to their original calibration site.

Another factor which seems to explain some of the differences between numerical wave models with $A + B$ source terms and the type described in this paper comes from the difference in the rate of propagation of the source terms themselves along a fetch. As shown in Resio and Vincent (1979), the G_{NL} source term propagates at the rate $C_g(f_m)$, whereas the A and B source terms propagate at the group velocities of the individual spectral elements. Table 1 from that study gives a comparison of the times required to achieve fetch limitation for the different types of models. It is shown there that models with $A + B$ source terms that grow correctly with time grow too slowly with fetch; and such models that grow correctly with fetch grow too fast with time.

The previous discussion suggests that numerical models with dominant $A + B$ source terms cannot duplicate similarity relationships observed in the JONSWAP data. Still, in a complete specification of source terms, it is necessary to include some explicit atmospheric input term. Most recent experiments indicate that the majority of the energy transfer from the atmosphere into the wave field occurs in the midrange of energy containing frequencies; and, since the theoretical form of the A term transfers more energy into spectral elements on the forward face of the spectrum than into this range, the A term is dropped entirely from the source terms in the present model. A simple form for B is used here, similar to that proposed by Snyder and Cox (1966)

TABLE 1. Comparison of durations (hours) required to achieve fetch-limited conditions in models dominated by atmosphere input source terms and in models dominated by wave-wave interaction source terms.*

Wind speed (kt)	Dominant source term	Fetch (n mi) 10	50	100	500
20	G_{AT}	2.3	6.9	11.3	31.4
	G_{NL}	3.2	9.4	14.9	44.0
40	G_{AT}	1.6	4.6	7.5	22.3
	G_{NL}	2.2	6.4	10.2	30.2
60	G_{AT}	1.6	4.2	7.2	23.1
	G_{NL}	1.9	5.5	8.8	26.0

* Assuming that both models produce values for f_m equal to those given by Hasselmann *et al.* (1976).

$$B_2 = sf[(u \cos\theta)c^{-1} - 0.9], \qquad (26)$$

where s is the ratio of the densities of air and sea water. This is equivalent to using the form of B_2 proposed by Barnett (1968) multiplied by 0.2. In Barnett's work, the $A + B$ terms were determined in such a way that they explained all of the wave growth along a fetch. A 4/5 reduction is consistent with more recent findings that ~80% of the growth is due to the wave-wave interaction source (Hasselmann *et al.*, 1973). The final form of the source terms used in this discrete spectral model is

$$S = G_{NL} + B_1 E(f)\psi(\theta - \theta_0). \qquad (27)$$

Since there is no longer any A term in this source formulation, a linear term to initiate wave growth is now lacking. It is apparent that waves must already be present in order to have wave-wave interactions which generate more waves. Consequently, it is necessary to have some high-frequency cutoff in such a discrete spectral model. In the model described here, this cutoff is achieved at a moderate frequency level by incorporating a local (nonpropagating) parametric model into the discrete spectral model. The boundary between the parametric and discrete spectral domains of this model is maintained at a fixed point, and energy in each domain is conserved independently. In a growing sea, energy is initiated in the parametric region. The rate of change of f_m is calculated and energy exchange into the discrete spectral region is used to trigger the growth in that domain. The calculation of a new f_m at the end of a time step in this model follows from the solution to the parametric equations of Hasselmann *et al.* (1976).

$$f_m^{n+1} = \left[\left(f_m^n\right)^{-7/3} + \frac{7}{3} N_v'\left(\frac{u}{g}\right)^{4/3} \Delta t\right]^{-7/3},$$

where the superscript n here denotes the time step, Δt is the time increment used in the model, and $N_v' = 0.00109 N_v$, where N_v is a constant specified by Hasselmann *et al.* (1976). Once the peak frequency has shifted into discrete spectral domain, the parametric domain assumes an f^{-5} equilibrium form.

5. Comparison to growth characteristics of Hasselmann *et al.* (1976) parametric model

The rate of wave growth under ideal conditions of fetch limitation or duration limitation under a stationary wind field can be calculated from the Hasselmann *et al.* (1976) study. For growth along a fetch, this solution yields

$$E_0 = 1.6 \times 10^{-7} u^2 x/g \tag{29}$$

and for growth through time, it becomes

$$E_0 = 4.3 \times 10^{-10} u^{18/7} g^{-4/7} t^{10/7}, \tag{30}$$

where t is the total elapsed time since the wind began to blow, assuming an initial condition of $E_0 = 0$ at $t = 0$.

In order to use Eq. (13) in actual calculations, the constant D_1 must be evaluated from comparisons to the complete solution. Fig. 4 shows the results of calculations of the parameterized wave-wave interactions based on the type of formulation given in Eq. (5). For the growth of a Kitaigorodskii-type spectrum, this is equivalent to Eq. (13) with $D_1 = 0.0023$. Clearly, the new parameterizations yield a more consistent source function relative to the complete solution. Without any recourse to recalibration, the discrete spectral model was run for ideal fetch- and duration-limited cases, assuming a Kitaigorodskii-type spectrum. Fig. 5 shows that results from these runs compare quite favorably to the parametric results.

In the parametric model, wave growth is automatically halted when the nondimensional peak frequency attains the value 0.13; and a fully developed sea state is achieved abruptly at this value. In the discrete spectral model a property of combined source terms can be shown to affect an asymptotic approach to a fully developed sea state, without requiring a side condition on the value of a parameter. Basically, the saturation range in the discrete spectral model is attained when the atmospheric input (B term) puts more energy into the central band of frequencies than is transferred out of this range of the wave-wave interactions. Whether the level of energy in this range is controlled by wave-wave interactions or by wave breaking is not really relevant in the present discussion provided both lead to an f^{-5} distribution of energy as empirical evidence suggests. Eventually as the negative lobe of the wave-wave interactions moves progressively into lower frequencies, it will approach the so-called wind frequency ($f = g/u$), at which point the B term goes to zero. When this occurs, the spectral shape becomes broader near the peak since it can no longer maintain an f^{-5} distribution, and the rate of wave growth slows down from the similarity-based relationships shown in Eqs. (29) and (30). Dimensional considerations indicate that such a condition on the wind frequency leads to a fully developed energy that depends on wind speed to the fourth power, i.e., $E_{\mathrm{SAT}} \sim u^4$. This is in agreement with empirical evidence which supports a wind speed squared relationship for fully developed wave height (Pierson and Moskowitz, 1964). The deviation between the discrete spectral model and the parametric model at large fetches and durations shown in Fig. 5 is probably due to the difference in their approaches to fully developed conditions.

6. Transition to swell and swell decay

In the parametric model, waves are said to be swell when the nondimensional peak frequency becomes <0.13. When this occurs in the parametric model, the spectral components are assumed to become instantaneously uncoupled and a discrete spectral propagation scheme, typically using the method of characteristics, is used to move the energy over the ocean surface at the group velocity of each individual frequency. Since the point of contact in frequency between the local sea and swell calculations is not fixed, there are a number of computational difficulties which must be overcome in order to maintain a smooth, stable solution. Since it is assumed that these spectral elements are completely uncoupled from each other, there is no decay of energy as the waves propagate away from their source. There is still geometric spreading and frequency dispersion which will reduce the energy density as one moves away from the source; but total energy is conserved.

In the discrete spectral model presented here, there is no difficulty in propagation brought about by mixed computational systems at the same frequency. Propagation is achieved for all spectral elements lower than the parametric high-frequency domain by using an explicit finite-difference formula

$$F_{ij}^{n+1} = \sum_{k=1}^{5} \lambda_k F_{ijk}^{n}, \tag{31}$$

where the superscript n denotes the time step in the model and subscripts i, j and k refer to frequency, direction and space counters, respectively. The values of the multipliers represent a one-step version of a modified Lax-Wendroff scheme used by Burridge and Gadd (1978) and Golding (1978). This scheme is space-centered and quasi-time centered, and is computed here on a nonstaggered grid. After

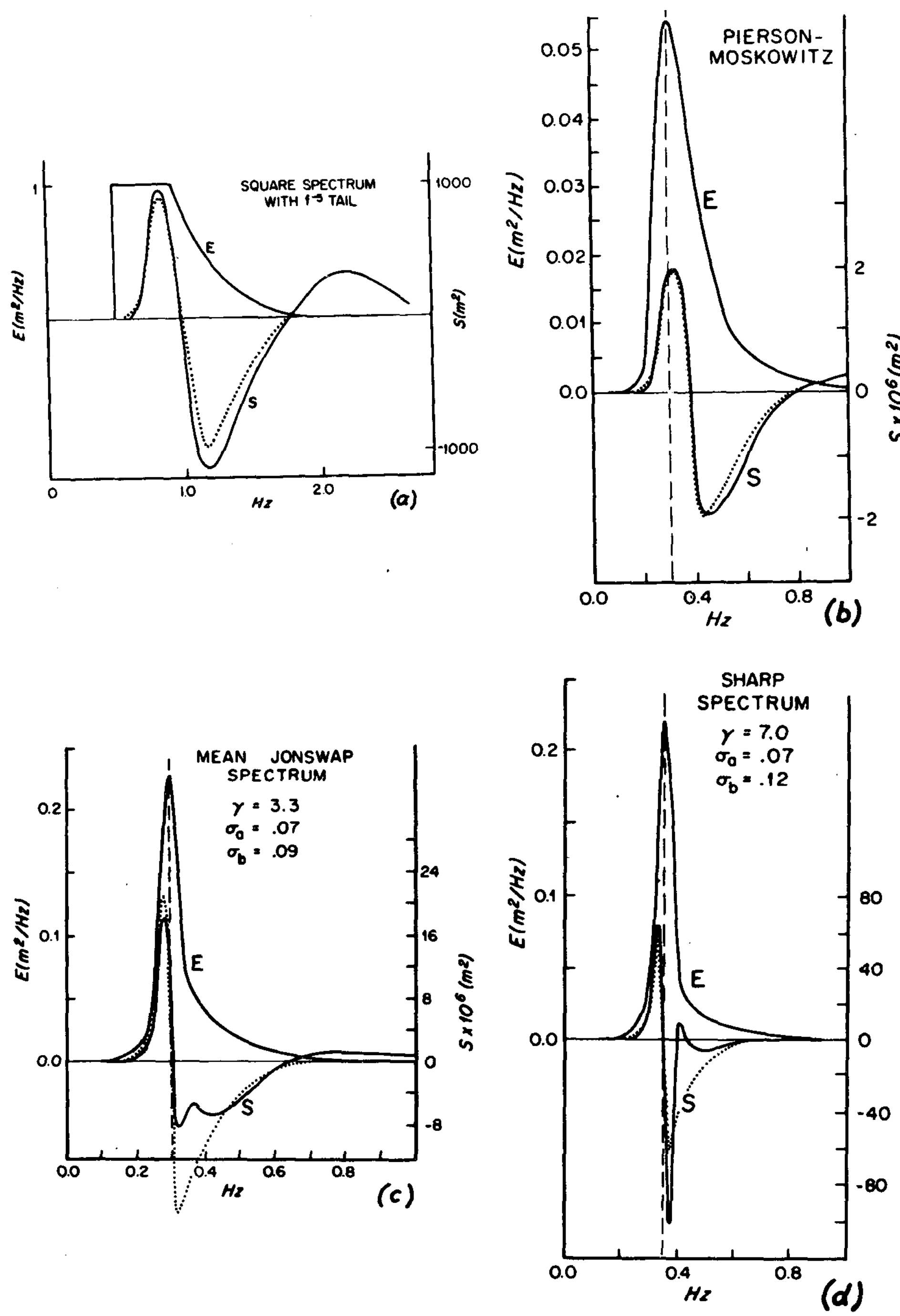

FIG. 4. Comparison of parameterizations of wave-wave interaction source terms based on equation in text to computed solutions of complete integrals (Hasselmann *et al.*, 1973).

the spectral peak of the locally generated waves is determined, the wave-wave interaction source for a swell spectrum is computed using the same concepts as used for the local sea and the total source integration is performed. Fig. 6 shows a typical decay sequence for a wave spectrum after the wind is switched off in the discrete spectral model. The lack of such an energy-decaying factor for swell in a purely parametric model could be a major drawback in its application for climatological processes. This is especially true for cases in which wave statistics are required for planning, design, operation and maintenance related to coastal structures or when otherwise used to quantify nearshore processes.

In the sequence of spectra shown in Fig. 6, the

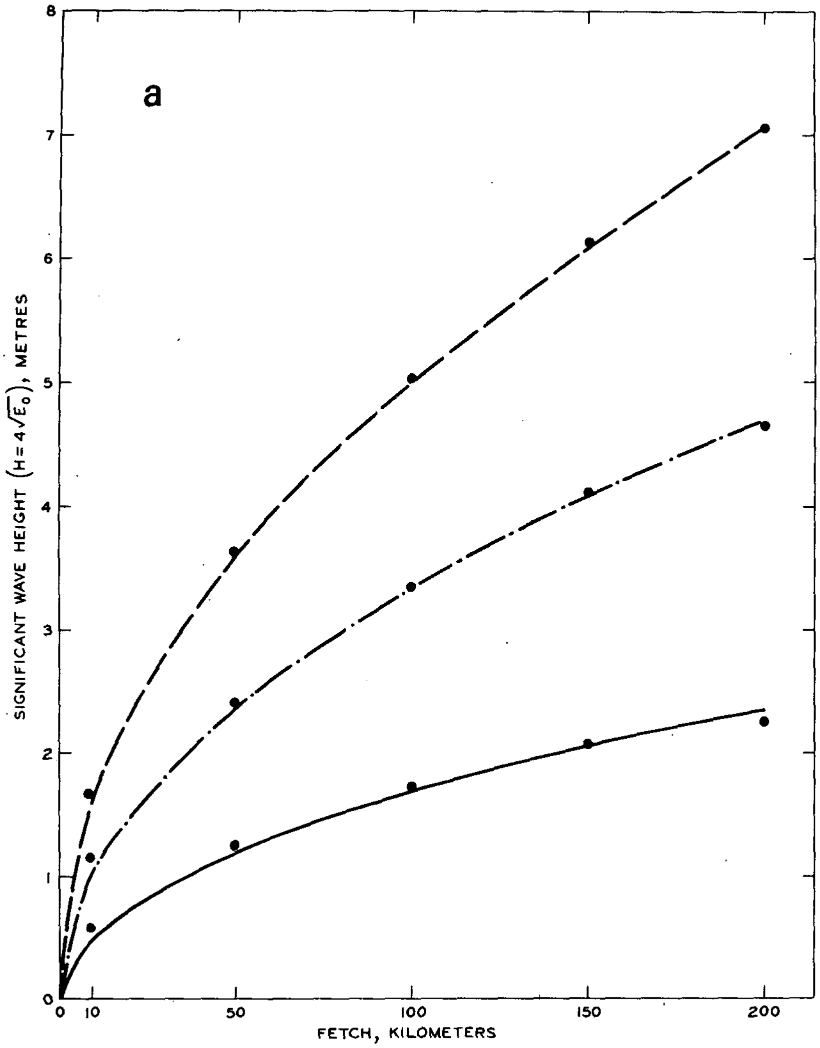

FIG. 5. Comparison of growth of wave height (a) along a fetch and (b) through time predicted by discrete spectral model to growth of wave height predicted by Hasselmann *et al.* (1976) parametric model.

negative lobe of the wave-wave interaction source is parameterized so as to maintain a constant f^{-5} slope at frequencies above the spectral peak. There is evidence from the field study of Snodgrass *et al.* (1966) and the laboratory study of Mitsuyasu and Kimura (1965) that this occurs in nature, at least in the region relatively close to the wave generation area. For computational simplicity, the form of the parameterization is given by

$$G_{\mathrm{NL}(-)} = (D_5/G^4)E^2(f_m)f_m^{11}E(f). \qquad (32)$$

This formula retains the basic α^3 dependence of the source function and is basically a substitution of $E(f)/E(f_m)$ for the function $\psi(f/f_m)$ in Eq. (5). After waves have propagated a large distance relative to the size of the wind system responsible for the wave generation, frequency dispersion will tend to produce very peaked swell spectra; however, at these distances the rate of energy decay becomes quite small (Snodgrass *et al.*, 1966). Thus, the deviation between the parameterized shape function, with the assumed f^{-5} high-frequency tail and actual spectral shapes should not be of major consequence.

7. Discussion

The model described in this paper represents a discrete spectral model that approximates the similarity-based fetch and duration growth characteristics of the Hasselmann *et al.* (1976) parametric model. At present, it is undergoing extensive testing against recorded wave spectra; however, since error characteristics in such a comparison are as much a product of the meteorological models used to estimate an oceanic wind field as the wave model, these results will not be reported here. The fundamental physics of the discrete spectral model consists of three parts: a new parameterization of the wave-

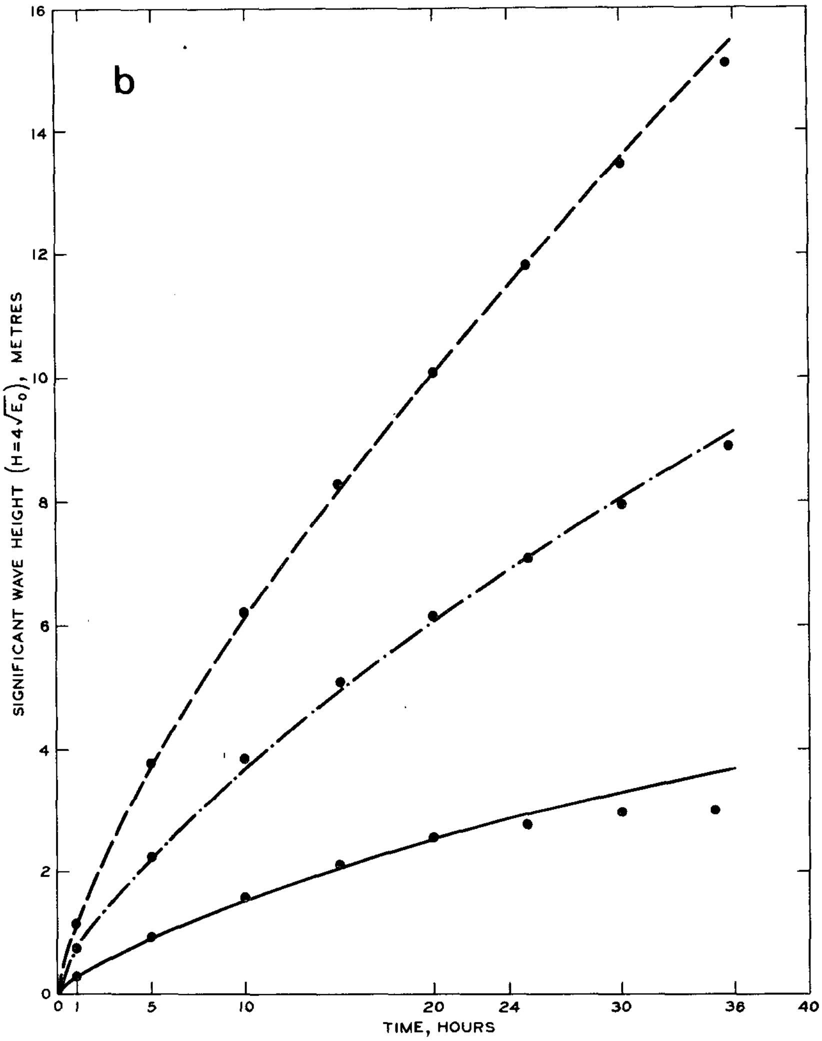

Fig. 5. (*Continued*)

wave interaction source term, an atmospheric input term of the exponential type and a variable energy density level in the range of frequencies above the spectral peak, where a balance of energy fluxes leads to an f^{-5} distribution of energy. It would appear from the results of this paper and that of Resio and Vincent (1979) that a model with dominant atmospheric input source terms cannot be scaled to match the results of the discrete spectral model with a dominant nonlinear wave-wave interaction source term.

On the other hand, the parametric model has some attributes which do not appear to be substantiated by observations. One of these, the lack of swell decay, is remedied in the discrete spectral model by maintaining the ability to calculate two sets of wave-wave interaction source terms, one for local sea and one for swell. A second problem area with the parametric model for many applications is the assumption that the wave spectrum is always centered around the wind angle. Hasselmann *et al.* (1976) use an argument based on the relaxation time of the value of α to justify this assumption. However, the region of frequencies in which this adjustment is rapid is above f_0. In this area, energy already present in the spectrum is transported out of this region, while the wind puts in additional energy toward its central direction. On the forward face of the spectrum, the adjustment to a shift in wind must be much slower, since no previously present energy is transported out of this region and the net wave-wave interaction source is centered around the central wave angle and not the wind direction. It is interesting to note here that, whereas a variable wind speed can be rescaled into a similarity process equivalent to a series of constant wind speeds with different initial conditions, this is not the case for a change in wind angle. The discrete spectral model can be shown to produce a spectrum under a changing wind angle with energy on the forward face propagating

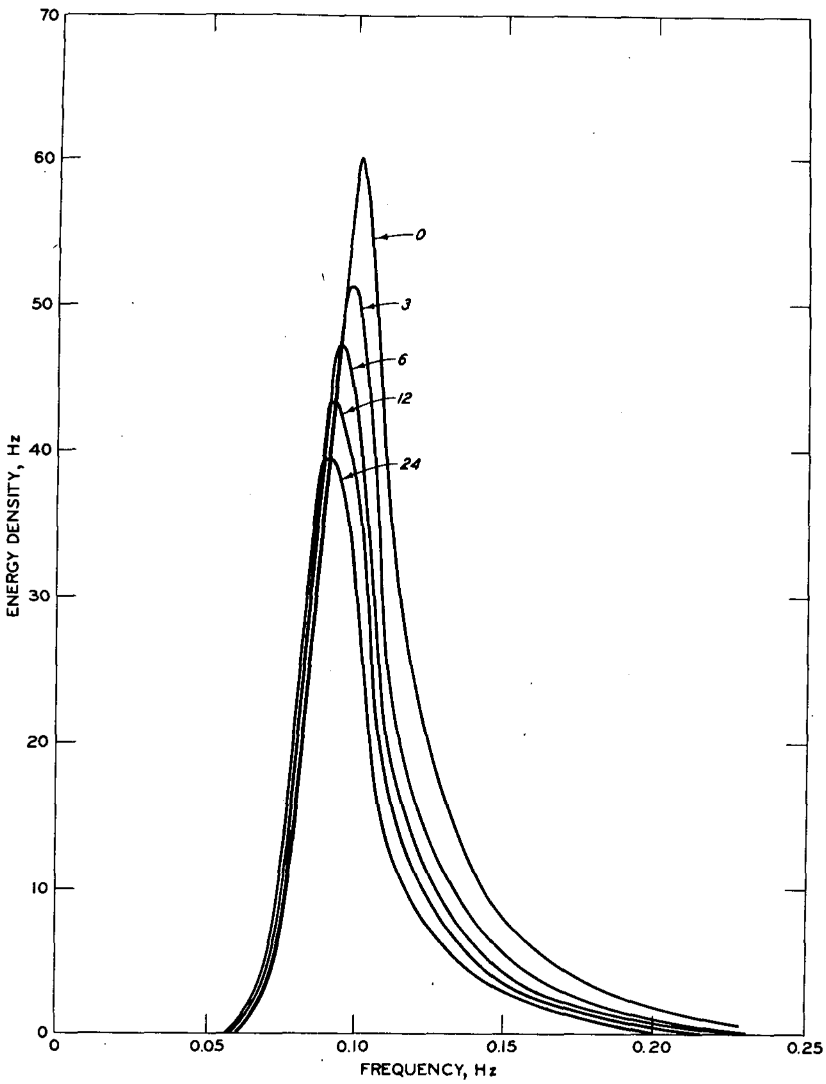

FIG. 6. Decay of a wave spectrum from time $t = 0$ to $t = 24$ h predicted by wave-wave interactions as parameterized in Eqs. (32) (negative lobe) and (13) (positive lobe).

in a significantly different direction than the energy at high frequencies. This type of deviation has been reported by Forristall *et al.* (1978) and in data from the GATE project.

In actual applications with the discrete spectral model described in this paper, better results have been achieved by using scaling relationships between α and nondimensional wave height that are based on friction velocity rather than wind speed at some reference level. This is in accordance with the original work of Kitaigorodskii (1962). Only if the coefficient of drag is constant will the two scalings produce identical results; and many papers in recent years have presented evidence that this is not the case for winds over water. Garrett (1977) summarizes the data and results of several studies and suggests a velocity dependence of the roughness length of the water's surface that is similar to Charnock's (1955) formulation $z_0 \sim u_*^2/g$. Since there is an algebraic relationship between the roughness length and the coefficient of drag, this relationship may be incorporated into the JONSWAP data in order to extend these data to the case of friction velocity scaling. Fig. 7 shows that this different scaling can produce significant differences even at wind speeds as low as 30 kt. As seen here, with the wind-speed scaling, the growth of wave height with time is considerably lower than other models (which have presumably been tuned to fit actual data); whereas, with the friction velocity scaling, the growth of wave height with time appears to fit in with the other models quite well.

If friction velocity is the more appropriate scaling parameter for wave generation, there also may be a dependence on atmospheric stability. Schwab (1978) reported that results from his numerical model of

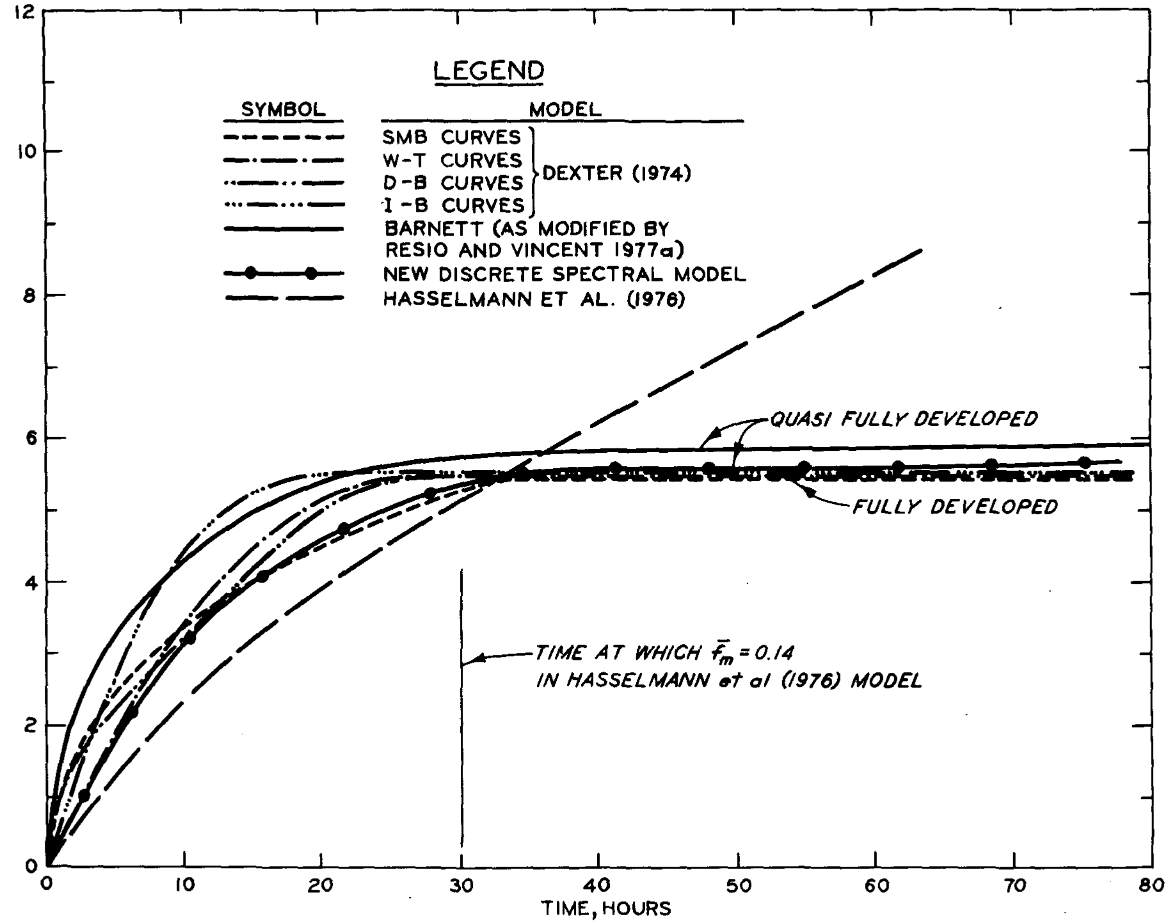

FIG. 7. Comparison of duration-limited wave growth predicted by Hasselmann *et al.* (1976) parametric model (scaled by wind velocity) and duration-limited wave growth predicted by discrete spectral model (scaled by friction velocity) to wave growth in duration limited cases in various other models.

wind stress over Lake Erie were improved when consideration of drag variation of the type presented by Resio and Vincent (1977b) was included. Also, Strong and Bellaire (1965), Davidson (1973), Sanders (1976) and Cardone (1969) present evidence that wave generation can be significantly influenced by atmospheric stability. If this is the case, then a friction velocity scaling will tend to give better agreement with observations when used in a climatological application.

Another factor which can be of significance in the application of a numerical wave model concerns the run time characteristics. A major argument against the use of discrete spectral models is the large amount of computer time and large area storage requirements necessary in the simulation of waves over a large area. In a 576-point Atlantic Ocean grid at each point, 320 spectral elements and a high-frequency parametric domain are used to represent the wave spectrum, giving a total of 184 320 elements in all. Source calculations are performed for these and each element is propagated, using Eq. (31). Speed is achieved by performing as many precalculations as possible and by minimizing branching logic. One day of simulation for the Atlantic (eight time steps) can be run in ~16 s on a CDC CYBER 176 computer. Thus, the run time is really not too great a factor for many potential applications even at the scale of the entire Atlantic Ocean. For a smaller number of points or a smaller number of frequency-direction elements, commensurately less run time will be required.

As a final part of this discussion, it is appropriate to include a comparison of the discrete spectral model to some recent wind-wave models other than the PTB type and Hasselmann *et al.* (1976) parametric model. In the last few years, the concept of a wave spectrum as a superposition of free surface waves has been challenged. Toba (1978) and Lake and Yuen (1978) argue that the wave spectrum is not weakly nonlinear, as suggested by Hasselmann (1962) but rather represents a strongly nonlinear process. Based on laboratory studies (Rikiishi, 1978; Kato and Tsuruya, 1974; Ramamonjiarisoa and Coantic, 1976), the group velocity of spectral components with frequencies higher than the spectral peak appears to deviate significantly from linear theory. Preliminary findings suggest instead that these waves are coupled to dominant waves, located at frequencies near the spectral peak, and propagate at the same group velocity as these waves. Lake and Yuen go on to explain this behavior and associated energy transfers within an evolving one-dimensional wave spectrum in terms of the nonlinear Schrödinger equation. The spectrum in this sense represents a coherent system of bound waves. In such a system, the interactions among frequencies are not restricted to those wavenumbers satisfying the resonance condition expressed by the delta functions in Eqs. (4a) and (4b).

In a wind-wave spectrum, this apparent propagation behavior of the high frequency components is not surprising. Since the equilibrium range is maintained by a balance of energy fluxes through this region of the spectrum, the level of energy here is a local quantity. As shown by Hasselmann *et al.* (1976), the relaxation time of the energy level in this region of the spectrum is very short. Like any local quantity, the integrity of individual waves is not maintained for long distances. A consequence of this is that propagation characteristics of high-frequency waves in a spectrum do not necessarily infer that all wave energy is bound to the dominant waves, but might reflect the local nature of these waves which in turn depend highly on the dominant waves present.

Laboratory studies (Lake *et al.*, 1977) also indicate that the form of a wave train in deep water evolves through a series of cycles of amplitude modulation, in agreement with the coupled form of the nonlinear Schrödinger equation. In this type of evolution, the spectrum alternately becomes more concentrated and then more dispersed in frequency, an apparent violation of the principle that entropy is a nondecreasing function. Herein lies a fundamental difference between the coupled mode behavior and the weakly nonlinear interactions. Whereas the latter of these is formulated in terms of wave action, which is averaged over phase, the former is not. In the random sea model, entropy can be measured by an equivalence to dispersion of energy in wavenumber space. In the bound wave model, the entropy of the system must be defined in terms of the probability that the system is in a particular portion of the phase space. Since high correlations can exist among different wave components in the bound wave system, this, too, must be considered as a contributor to total entropy. Hence, the redistribution of the spectral energy undergoing amplitude modulation must be accompanied by a counterbalancing redistribution of the correlation structure in such a way as to negate the apparent decrease in entropy. In the basically one-dimensional case typical of a wave confined in a flume, it is expected that considerably higher correlation among different components can be maintained then when waves are free to propagate at varying angles to each other. This does not lead to a definite conclusion as to which model of the physics is more appropriate in prototype conditions. However, since both models produce a growing spectrum with an f^{-5} high-frequency region and a source function linked to the location of the spectral peak, use of either model when empirical evidence is also considered, must inevitably lead to similar results.

8. Summary and conclusions

A discrete spectral model has been presented which exhibits fetch and duration growth characteristics to the Hasselmann *et al.* (1976) parametric model. Source terms with a dominant atmospheric input apparently cannot duplicate these growth characteristics. The parameterization of the wave-wave interaction source term by Barnett (1968) was seen to be too low by a factor of 3 for a JONSWAP spectrum; consequently, a new parameterization was formulated for the wave-wave interaction source terms. This parameterization can account for certain aspects of spectral shape variation and leads to a simple $\alpha^3 f_m^{-4}$ scaling relationship for the nonlinear source term in a self-similar spectrum with an f^{-5} high-frequency tail. This type of source representation is found to depict both wave growth and wave decay rates in accordance with observational evidence while maintaining spectral shapes consistent with observed spectra. Advantages over a parametric model include simplified numerics since only one computational system is used for sea and swell, the ability to represent swell decay as it propagates away from a storm area, and the freedom to permit wave direction to deviate from wind direction in situations of rapidly varying wind directions.

Acknowledgments. I would like to thank the U.S. Army Engineer Waterways Experiment Station for permission to publish this manuscript and the Office of the Chief for sponsoring the project on which this work was accomplished. I would also like to thank Dr. C. L. Vincent for many excellent discussions of materials covered in this paper and contributions to the model described.

REFERENCES

Barnett, T. P., 1968: On the generation, dissipation, and prediction of wind waves. *J. Geophys. Res.*, **73**, 513–529.

——, and A. J. Sutherland, 1968: A note on the over-shoot effect in wind-generated waves. *J. Geophys. Res.*, **73**, 6897–6885.

Burridge, D. M., and A. J. Gadd, 1978: The Meteorological Office operational 10-level numerical weather prediction model. (Dec. 1975). Meteorological Office, Sci. Pap. No. 34, HMSO, 39 pp.

Cardone, V. J., 1969: Specification of the wind distribution in the

marine boundary layer for wave forecasting. Tech. Rep. 69-1, Geophys. Sci. Lab., New York University, 137 pp.
——, and D. B. Ross, 1977: State-of-the-art wave prediction methods and data requirements. *Ocean Wave Climate*, M. Earle, Ed., Plenum Press, 61–91.
Charnock, H., 1955: Wind stress on a water surface. *Quart. J. Roy. Meteor. Soc.*, **81**, 639–640.
Davidson, K. L., 1974: Observational results on the influence of stability and wind-waves coupling on momentum transfer and turbulent fluctuations over ocean waves. *Bound.-Layer Meteor.*, **6**, 305–331.
Dexter, P. E., 1974: Tests of some programmed numerical wave forecast models. *J. Phys. Oceanogr.*, **4**, 635–644.
Dobson, F. W., 1971: Measurements of atmospheric pressure on wind-generated sea waves. *J. Fluid Mech.*, **48**, 91–127.
——, and J. A. Elliot, 1978: Wave-pressure correlation measurements over growing sea waves with a wave follower and fixed-height pressure sensors. *Turbulent Fluxes Through the Sea Surface, Wave Dynamics, and Predictions*, A. Favre and K. Hasselmann, Eds., Plenum Press, 421–432.
Ewing, J. A., 1971: A numerical wave prediction method for the North Atlantic Ocean. *Dtsch. Hydrogr. Z.*, **24**, 241–261.
Forristall, G. Z., E. G. Ward, V. J. Cardone and L. E. Borgman, 1978: The directional spectra and kinematics of surface gravity waves in Tropical Storm Delia. *J. Phys. Oceanogr.*, **8**, 888–909.
Garrett, J. R., 1977: Review of drag coefficients over oceans and continents. *Mon. Wea. Rev.*, **105**, 915–929.
Golding, B. W., 1978: A depth-dependent wave model for operational forecasting. *Turbulent Fluxes Through the Sea Surface, Wave Dynamics, and Predictions*, A. Favre and K. Hasselmann, Eds., Plenum Press, 593–606.
Hasselmann, K., 1962: On the non-linear energy transfer in a gravity-wave spectrum—general theory. *J. Fluid Mech.*, **12**, Part 1, 481–500.
——, T. P. Barnett, E. Bouws, H. Carlson, D. E. Cartwright, K. Enke, J. A. Ewing, H. Gienapp, D. E. Hasselmann, P. Kruseman, A. Meerburg, P. Muller, D. J. Olbers, K. Richter, W. Sell and H. Walden, 1973: Measurements of wind-wave growth and swell decay during the Joint North Sea Wave Project JONSWAP. *Dtsch. Hydrogr. Z.*, **8** (Suppl. A8), No. 12, 95 pp.
——, D. B. Ross, P. Muller and W. Sell, 1976: A parametric wave prediction model. *J. Phys. Oceanogr.*, **6**, 200–228.
Kato, H., and K. Tsuruya, 1974: On the phase velocity of component waves of wind waves. *Proc. 21st Japan Conf. Coastal Engineering*, Japan Soc. Civil Engr., 255–259.
Kitaigorodskii, S. A., 1962: Application of the theory of similarity to the analysis of wind-generated wave motion as a stochastic process. *Bull. Acad. Sci. USSR Ser. Geophys.*, No. 1, Vol. 1, 105–117.
Lake, B. M., and H. C. Yuen, 1978: A new model for nonlinear wind waves. Part 1. Physical model and experimental evidence. *J. Fluid Mech.*, **88**, 33–62.
——, ——, H. Rungaldier and W. E. Ferguson, 1977: Nonlinear deep-water waves: Theory and experiment. Part 2. Evolution of a continuous wave train. *J. Fluid Mech.*, **83**, 49–74.
Lazanoff, S. M., and N. M. Stevenson, 1975: An evaluation of a hemispheric operational wave spectral model. U.S. Navy Fleet Numerical Weather Central, Tech. Note 75-3, 103 pp.
Liu, P. C., 1971: Normalized and equilibrium spectra of wind waves in Lake Michigan. *J. Phys. Oceanogr.*, **1**, 249–257.
Miles, J. W., 1957: On the generation of surface waves by shear flows. *J. Fluid Mech.*, **3**, 185–204.
Mitsuyasu, H., 1968: On the growth of wind-generated waves (I). *Rep. Res. Inst. Appl. Mech., Kyushu Univ.*, **16**, 459–482.
——, 1969: On the growth of the spectrum of wind-generated waves (II). *Rep. Res. Inst. Appl. Mech., Kyushu Univ.*, **27**, 235–248.
——, and H. Kimura, 1965: Wind wave in decay area. *Coast Engr. Japan*, **8**, 21–35.
Phillips, O. M., 1957: On the generation of waves by turbulent wind. *J. Fluid. Mech.*, **2**, 417–445.
Pierson, W. J., 1977: Comments on "A parametric wave model." *J. Phys. Oceanogr.*, **7**, 127–134.
——, and L. Moskowitz, 1964: A proposed spectral form for fully developed wind seas based on the similarity theory of S. A. Kitaigorodskii. *J. Geophys. Res.*, **69**, 5181–5190.
——, L. J. Tick and L. Baer, 1966: Computer based procedures for preparing global wave forecasts and wind field analyses capable of using wave data obtained by a spacecraft. *Proc. Sixth Naval Hydrodynamics Symp.*, 499–532.
Ramamonjiarisoa, A., and M. Coantic, 1976: Loi experimentale de dispersion des vagues produites par le vent sur uni faible longueur d'action. *C.R. Acad. Sci. Paris*, **B282**, 111–113.
Resio, D. T., and C. L. Vincent, 1977a: A numerical hindcast model for wave spectra on water bodies with irregular shoreline geometry, Report 1: Test of nondimensional growth rates. Misc. Paper H-77-9, Hydraulics Lab., U.S. Army Engineer Waterways Experiment Station, 53 pp.
——, and ——, 1977b: Estimation of the winds over the Great Lakes. *ASCE J. Waterway Port Coast. Ocean Div.*, **103**, 265–283.
——, and ——, 1979: A comparison of various numerical wave prediction techniques. Presented at Offshore Technology Conf., Houston, Mar. Tech. Soc. and Amer. Soc. Civ. Eng., Pap. 3642.
Rikiishi, K., 1978: A new method for measuring the directional spectrum and phase velocity of laboratory wind waves. *J. Phys. Oceanogr.*, **8**, 518–529.
Sanders, J. W., 1976: A growth-state scaling model for the wind-driven sea. *Dtsch. Hydrogr. Z.*, **4**, 136–161.
Schwab, D. J., 1978: Simulation and forecasting of Lake Erie storm surges. *Mon. Wea. Rev.*, **106**, 1476–1487.
Synder, R., and C. S. Cox, 1966: A field study of the wind generation of ocean waves. *J. Mar. Res.*, **24**, 141–177.
Snodgrass, F. E., G. W. Groves, K. F. Hasselmann, G. R. Miller, W. H. Munk and W. H. Powers, 1966: Propagation of ocean swell across the Pacific. *Phil Trans. Roy. Soc. London*, **A259**, 431–497.
Strong, A. E., and F. R. Bellaire, 1965: The effect of air stability on wind and waves. Publ. No. 13, Great Lakes Res. Div., University of Michigan, 283–289.
Sverdrup, H. U., and W. H. Munk, 1947: Wind, sea, and swell: Theory of relations for forecasting. H.O. Publ. No. 601, U.S. Navy Hydrographic Office, Washington, DC, 44 pp.
Toba, Y., 1978: Stochastic form of the growth of wind waves in a single-parameter representation with physical implications. *J. Phys. Oceanogr.*, **8**, 494–507.
Weare, T. J., and B. Worthington, 1978: A numerical model of hindcast severe wave conditions for the North Sea. *Turbulent Fluxes Through the Sea Surface, Wave Dynamics and Prediction*, A Favre and K. Hasselmann, Eds., Plenum Press, 617–628.
Webb, D. J., 1978: Non-linear transfers between sea waves. *Deep-Sea Res.*, **25**, 279–298.
Wu, H-Y., E-Y. Hsu and R. L. Street, 1979: Experimental study of nonlinear wave-wave interaction and white-cap dissipation of wind-generated waves. *Dyn. Atmos. Oceans*, **3**, 55–78.